J Mater Sci (2011) 46:629–633
DOI 10.1007/s10853-010-4784-x

Molecular dynamics calculations of InSb nanowires thermal conductivity

Giovano de Oliveira Cardozo · José Pedro Rino

Received: 8 October 2009 / Accepted: 21 July 2010 / Published online: 10 August 2010

Abstract Non-equilibrium molecular dynamics calculations were performed in order to obtain the thermal conductivity coefficients of InSb nanowires in comparison with the bulk system value. For bulk, the value obtained was 16 ± 2 Wm^{-1} K^{-1} which is in very good agreement with experimental value of 15 Wm^{-1} K^{-1}, and the thermal conductivity of the nanowires were 0.54 ± 0.01 Wm^{-1} K^{-1} and 0.50 ± 0.01 Wm^{-1} K^{-1} for a 5 and 4 unit cells square cross-sectional nanowires, respectively, which is almost two orders of magnitude smaller. This result is in agreement with other simulations performed for other materials.

Introduction

Thermal conductivity in nanometrical systems is a subject of great interest in materials science and engineering. With the miniaturization of devices reaching nanometrical scales, it became very important to know how heat transport occurs in systems whose dimensions are of this order. This issue is particularly important for electronic devices, such as microprocessors, where the temperature must remain at low values to guarantee maximum performance and minimum energy consumption.

In the last few years a significant number of papers have been published with respect to thermal properties in nanosystems, like nanowires, nanorods, or nanotubes, of a variety of materials such as Si [1–8], Si/Ge [9], GaN [10], C [11, 12], and SiC [13]. Previous results show that for systems with small dimensions the thermal conductivity coefficient diminishes with the system diameter. This effect can be explained by the phonon surface roughness scattering [3, 14–16].

Indium antimonide (InSb), in particular, is a material with various important applications such as fast transistors (actually much faster than silicon ones and with lower energy consumption) [17] and thermal sensors for imaging devices [18]. In these devices an extremely efficient heat removal scheme is mandatory to maintain the temperature low, avoiding damages and keeping high performance.

In this article, we investigate the thermal conduction of InSb nanowires using non-equilibrium molecular dynamics simulations (NEMD). The results show that the InSb nanowires also present significant reduction in thermal conductivity coefficient in comparison with bulk thermal transport at room temperature.

The potential function

The potential function used here is a sum of the contributions of two- and three-body interactions. The pair potential part is composed of Coulomb, steric repulsion, charge-dipole, and dipole–dipole interactions. The three-body interactions consider bond bend and bond stretching effects.

The total energy interatomic potential is expressed by relation (1)

$$\Phi = \sum_{i<j} \varphi_{ij}^{(2)}(r_{ij}) + \sum_{i,j<k} \varphi_{jik}^{(3)}(r_{ij}, r_{ik}) \tag{1}$$

where

$$\varphi_{ij}^{(2)}(r) = \frac{H_{ij}}{r^{\eta_{ij}}} + \frac{Z_i Z_j}{r} e^{-r/\lambda} - \frac{D_{ij}}{2r^4} e^{-r/\xi} - \frac{W_{ij}}{r^6} \tag{2}$$

G. de Oliveira Cardozo (✉) · J. P. Rino
Departamento de Física, Universidade Federal de São Carlos, Via Washington Luiz km 235, 13565-905 São Carlos, SP, Brazil
e-mail: giovano@df.ufscar.br

and

$$\varphi^{(3)}_{jik}(r_{ij}, r_{ik}) = R^{(3)}(r_{ij}, r_{ik}) \cdot P^{(3)}(\theta_{jik}) \tag{3}$$

$$R^{(3)}(r_{ij}, r_{ik}) = B_{jik} \exp\left(\frac{\gamma}{r_{ij} - r_0} + \frac{\gamma}{r_{ik} - r_0}\right) \times \Theta(r_0 - r_{ij})\Theta(r_0 - r_{ik}) \tag{4}$$

$$P^{(3)}(\theta_{jik}) = \frac{\left(\cos\theta_{jik} - \cos\bar{\theta}_{jik}\right)^2}{1 + C_{jik}\left(\cos\theta_{jik} - \cos\bar{\theta}_{jik}\right)^2} \tag{5}$$

The two-body term of the potential is truncated at r_{cut} and shifted for $r < r_{\text{cut}}$ in order to have the value and its first derivative continuous at the cutoff distance [19, 20]. The shifted pair potential is given by

$$\varphi^{(2\text{shifted})}_{ij}(r) = \begin{cases} \varphi^{(2)}_{ij}(r) - \varphi^{(2)}_{ij}(r_{\text{cut}}) - (r - r_{\text{cut}})\left(\mathrm{d}\varphi^{(2)}_{ij}(r)\Big/\mathrm{d}r\right)_{r=r_{\text{cut}}} & r \le r_{\text{cut}} \\ 0 & r > r_{\text{cut}} \end{cases}$$

where $r \equiv r_{ij} = \left|\vec{r}_i - \vec{r}_j\right|$ represents the distance between atoms i and j, located at the positions $\vec{r}_i$ and $\vec{r}_j$, respectively, and λ and ξ are the screening lengths for Coulomb and charge-dipole terms, θ_{jik} the angle formed by $\vec{r}_{ij}$ and $\vec{r}_{ik}$, and C_{jik} and $\bar{\theta}_{jik}$ are constants, and $\Theta(r_0 - r_{ij})$ is a step function.

These interatomic potential, which was developed by Nakano et al. [21], is very transferable. The parameterization of the interatomic potential for InSb was done by Costa et al. [22, 23] and recently improved by Rino et al. [24].

Methodology

NEMD and Fourier law

To obtain the thermal conductivity coefficient in the NEMD simulations a temperature gradient is imposed on the system by hot and cold reservoirs, where the temperatures are forced to be constant and different from each other. Hot and cold reservoirs are separated by a distance L. The temperatures of the reservoirs are maintained constant by periodically rescaling particle velocities inside them. The temperature rescaling in the hot reservoir corresponds to an energy addition to the system, and in the cold reservoir an energy subtraction. In the stationary regime the average added energy must be equal to the subtracted one [25–27], and as a response emerges a heat current j through the system, given by relation (6), where δt is the time interval between two rescaling events, and A is the system cross-sectional area.

$$j = \frac{\Delta\varepsilon}{2A\delta t} \tag{6}$$

The temperature gradient, in stationary regime, is linear between reservoirs, and its slope ∇T can be easily calculated. The thermal conductivity coefficient is then obtained by using the Fourier law, given by relation (7).

$$\kappa = \frac{j}{\nabla T} \tag{7}$$

When periodic boundary conditions are imposed along the heat current direction, the heat can travel in two directions, as can be seen in Fig. 1, and for that reason the energy increment is divided by 2 in relation (6).

In this kind of calculation there is a strong finite size effect over the thermal conductivity coefficient, which is produced by the interactions between heat source and sink interfaces [28]. These interactions diminish as the distance L, between reservoirs, is increased, and vanish only in the case of an infinite system. As an infinite system is impossible inside a computational simulation, it is necessary to make an infinite extrapolation by calculating the thermal conductivity coefficient for systems with different sizes. It is shown in ref. [28] that the inverse of thermal conductivity coefficient is a linear function of the inverse of L, so that the coefficient of thermal conductivity can be obtained by plotting $1/k$ as a function of $1/L$ and fitting the points by a linear function whose linear coefficient is an approach to the inverse of the coefficient for an infinite system.

The systems under investigation

The systems simulated here were the bulk one and two nanowires with different square cross section of side H. Each one of these systems was constructed in five different lengths, measured in unit cells unities. The shortest system used was 50 unit cells long, followed by those of 80, 200,

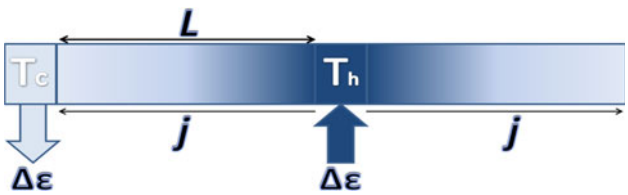

Fig. 1 System scheme for non-equilibrium calculation of thermal conductivity coefficient. T_c and T_h are, respectively, the temperatures of the cold and hot reservoirs

400, and 640 unit cells, respectively. The two values of H used were 5 and 4 unit cells, respectively (values which correspond to 3.2365 and 2.5892 nm). The bulk system was constructed with the same dimensions of the 5 unit cells diameter nanowire, differing from it by the existence of periodic boundary conditions in all directions, while the nanowires had it only along L direction, leaving free surfaces in the other two directions. In all of the systems the temperatures of the reservoirs were fixated at 350 and 250 K for the hot and cold ones, respectively, which resulted in a mean temperature of 300 K for the whole system. The zinc-blende nanowires InSb structures have the x-direction along [100] with surfaces along (001) and (010).

Simulations and results

The simulations started always with the equilibration of the bulk system, where an arbitrary number of molecular dynamics time steps were performed, in the micro-canonical (NVE) ensemble, to guarantee that the system is in equilibrium at a mean temperature of 300 K. After this procedure the nanowires were constructed by the addition of vacuum in the directions perpendicular to the system length, creating the surfaces. The nanowires were thermalized, in the canonical (NVT) ensemble at 300 K, with a number of MD steps enough to stabilize its structure. We observed that the surfaces rearrange but the whole nanowires keeps this form and is stable. Figure 2 depicted the stabilized nanowire at 300 K after the system being thermalized by 10,000 time steps. Once the structure became stable, the simulations returned to be made in NVE ensemble, the reservoirs were turned on and their temperature started to be corrected at every 1,000 simulation steps. After some temperature corrections, when the system reached the stationary regime, the temperature gradient became linear. At this point a long run of 10^6 time steps was performed, resulting in 10^3 temperature corrections in reservoirs. After that, the simulation was stopped and the average values of the energy increments were calculated. Figure 3 displays the temperature gradient between reservoirs in the stationary regime.

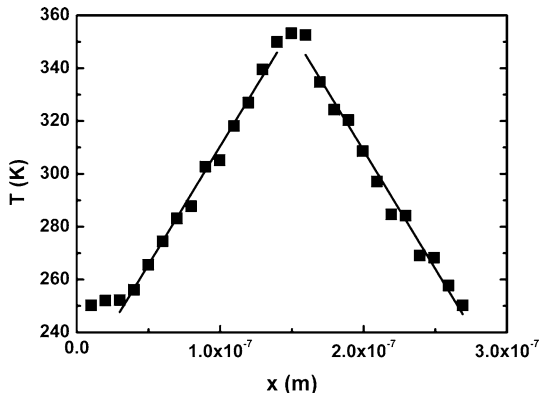

Fig. 3 System temperature in stationary regime as a function of the position. As expected, the temperature is a linear function of the position

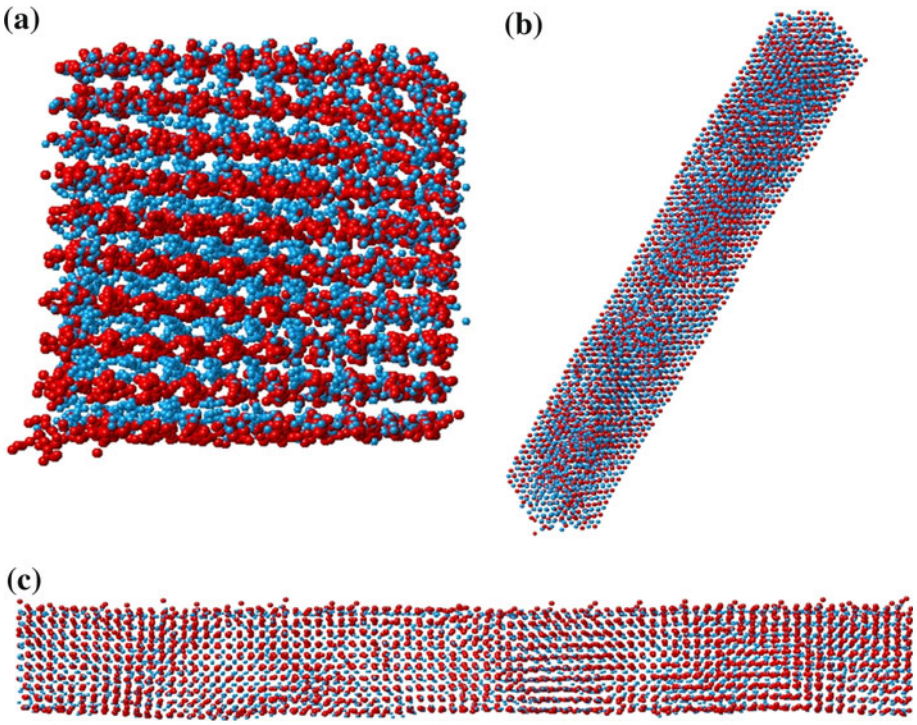

Fig. 2 (Color online) Nanowire in detail, showing that the surfaces are stable after the thermalization of the system. **a** (100) view, **b** (111) view, and **c** (101) view

In Fig. 4 the absolute average value of the energy increments in reservoirs shows that the energy added in the system is equal to that subtracted when the system is in the stationary regime.

In Fig. 5 the inverse of thermal conductivity coefficients against the inverse of the system length shows that as the system diameter decreases, the thermal conductivity coefficients also decrease. The bulk system, represented by the red line with circles (color online), resulted in a thermal conductivity coefficient of 16 ± 2 Wm^{-1} K^{-1} (in very good agreement with the experimental value of 15 Wm^{-1} K^{-1} [29, 30]) while the nanowire with a 5-unit cells side square cross section, represented by the blue line with triangles, resulted in a 0.54 ± 0.01 Wm^{-1} K^{-1} coefficient, almost two orders of magnitude smaller than the bulk, which is in accordance with previous simulations for other materials [9, 31]. The thermal coefficient from the 4-unit cells wide nanowire is even smaller, about 0.50 ± 0.01 Wm^{-1} K^{-1}, showing that the decrease in system diameter, with the correspondent increase in surface per volume ratio, increases the intensity of phonon scattering and consequently diminishes the heat transfer.

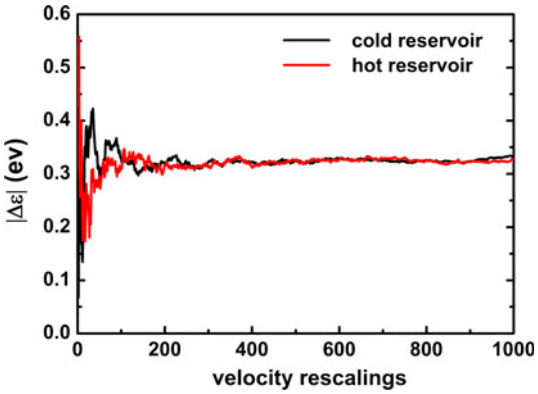

Fig. 4 (Color online) Energy added and subtracted for each reservoir as a function of the rescaled velocity. The average value of the energy increments in reservoirs converge to the same value in stationary regime

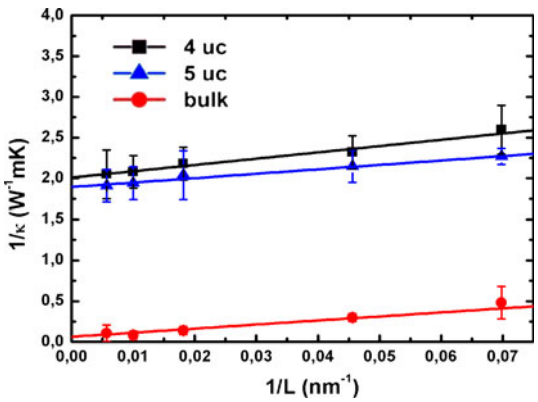

Fig. 5 (Color online) Inverse of thermal conductivity coefficient as a function of the inverse of the system length for bulk (*red line with circles*), and for nanowires with square cross-sectional widths of 5 unit cells (*blue line with triangles*) and 4 unit cells side (*black line with squares*)

Conclusions

We have presented a molecular dynamical study of thermal conductivity on InSb, bulk, and nanowires. As the heat transport is almost totally made by phonons in InSb at room temperature, any phenomenon which alters the phonon dynamics into the system can significantly change the heat conduction. For nanowires, the creation of free surfaces in the system also generated certain roughness which scattered the phonons in a way that the phonon–phonon interactions were dramatically affected. In this scenario the expected result was a significant decrease in heat transfer, reflected by a drastically lower thermal conductivity coefficient. This is exactly what was obtained by the simulations reported in this article. The results show that for the InSb, the thermal conductivity of the nanowire of 5-unit cells side square cross section is almost two orders of magnitude smaller than the bulk result (0.54 ± 0.01 against 16 ± 2 Wm^{-1} K^{-1} obtained for bulk). For a nanowire even thinner, of 4-unit cells side square cross section, where the surface is even more significant in the system, the obtained thermal conductivity coefficient, as expected, was also even smaller (0.50 ± 0.01 Wm^{-1} K^{-1} in comparison with 0.54 ± 0.01 Wm^{-1} K^{-1}). For bulk system the thermal conductivity coefficient agrees very well with experimental reported values. In conclusion, the proposed interatomic potential is very robust and can describe with confidence the properties of the indium antimonite material.

Acknowledgement This study was supported by CNPq, FAPESP, and CAPES.

References

1. Ju YS (2005) Appl Phys Lett 87:153106. doi:10.1063/1.2089178
2. Bourgeois O, Fournier T, Chaussy J (2007) J Appl Phys 101:016104. doi:10.1063/1.2400093
3. Chen R, Hochbaum AI, Murphy P, Moore J, Yang PD, Majumdar A (2008) Phys Rev Lett 101:105501. doi:10.1103/PhysRevLett.101.105501
4. Li D, Wu Y, Kim P, Shi L, Yang P, Majumdar A (2003) Appl Phys Lett 83:2934
5. Lu X (2008) J Appl Phys 104:054314. doi:10.1063/1.2976314
6. Lu X, Chu J (2006) J Appl Phys 100:014305. doi:10.1063/1.2211648
7. Mingo N, Yang L, Li D, Majumdar A (2003) Nano Lett 3:1713

8. Ponomareva I, Srivastava D, Menon M (2007) Nano Lett 7:1155. doi:10.1021/nl062823d
9. Li DY, Wu Y, Fan R, Yang PD, Majumdar A (2003) Appl Phys Lett 83:3186. doi:10.1063/1.1619221
10. Guthy C, Nam CY, Fischer JE (2008) J Appl Phys 103:064319. doi:10.1063/1.2894907
11. Fujii M, Zhang X, Xie HQ et al (2005) Phys Rev Lett 95:065502. doi:10.1103/PhysRevLett.95.065502
12. Padgett CW, Shenderova O, Brenner DW (2006) Nano Lett 6:1827. doi:10.1021/nl060588t
13. Papanikolaou N (2008) J Phys Condens Matter 20:135201. doi:10.1088/0953-8984/20/13/135201
14. Martin P, Aksamija Z, Pop E, Ravaioli U (2009) Phys Rev Lett 102(12):125503
15. Hochbaum AI, Chen R, Delgado RD et al (2008) Nature 451:163
16. Boukai AI, Bunimovich Y, Tahir-Kheli J, Yu J, Goddard WA III, Heath JR (2008) Nature 451:168
17. Intel (2005) Intel News Release
18. Avery DG, Goodwin DW, Rennie AE (1957) J Sci Instrum 34(10):394
19. Allen MP, Tildesley DJ (1987) Computer simulation of liquids. Oxford University Press, Oxford
20. Nakano A, Kalia RK, Vashishta P (1994) Comput Phys Commun 83:197
21. Nakano A, Kalia RK, Vashishta P (1994) J Non-Cryst Solids 171(2):157
22. Costa SC, Pizani PS, Rino JP (2003) Phys Rev B 68:073204. doi:10.1103/PhysRevB.68.073204
23. Costa SC, Pizani PS, Rino JP (2002) Phys Rev B 66:214111. doi:10.1103/PhysRevB.66.214111
24. Rino JP, de Oliveira Cardozo G, Picinin A (2009) CMC: Comput Mater Con 12(2):145
25. Baranyai A (1996) Phys Rev E 54:6911
26. Baranyai A (2000) Phys Rev E 62:5989
27. Baranyai A (2001) J Chem Phys 115:4156
28. Schelling PK, Phillpot SR, Keblinski P (2002) Phys Rev B 65:144306. doi:10.1103/PhysRevB.65.144306
29. Busch G, Steigmeier E (1961) Helv Phys Ada 34:1
30. Magomedov YB, Bilalov AR (2001) Semiconductors 35:499
31. Carrete J, Longo RC, Varela LM, Rino JP, Gallego LJ (2009) Phys Rev B 80:155408